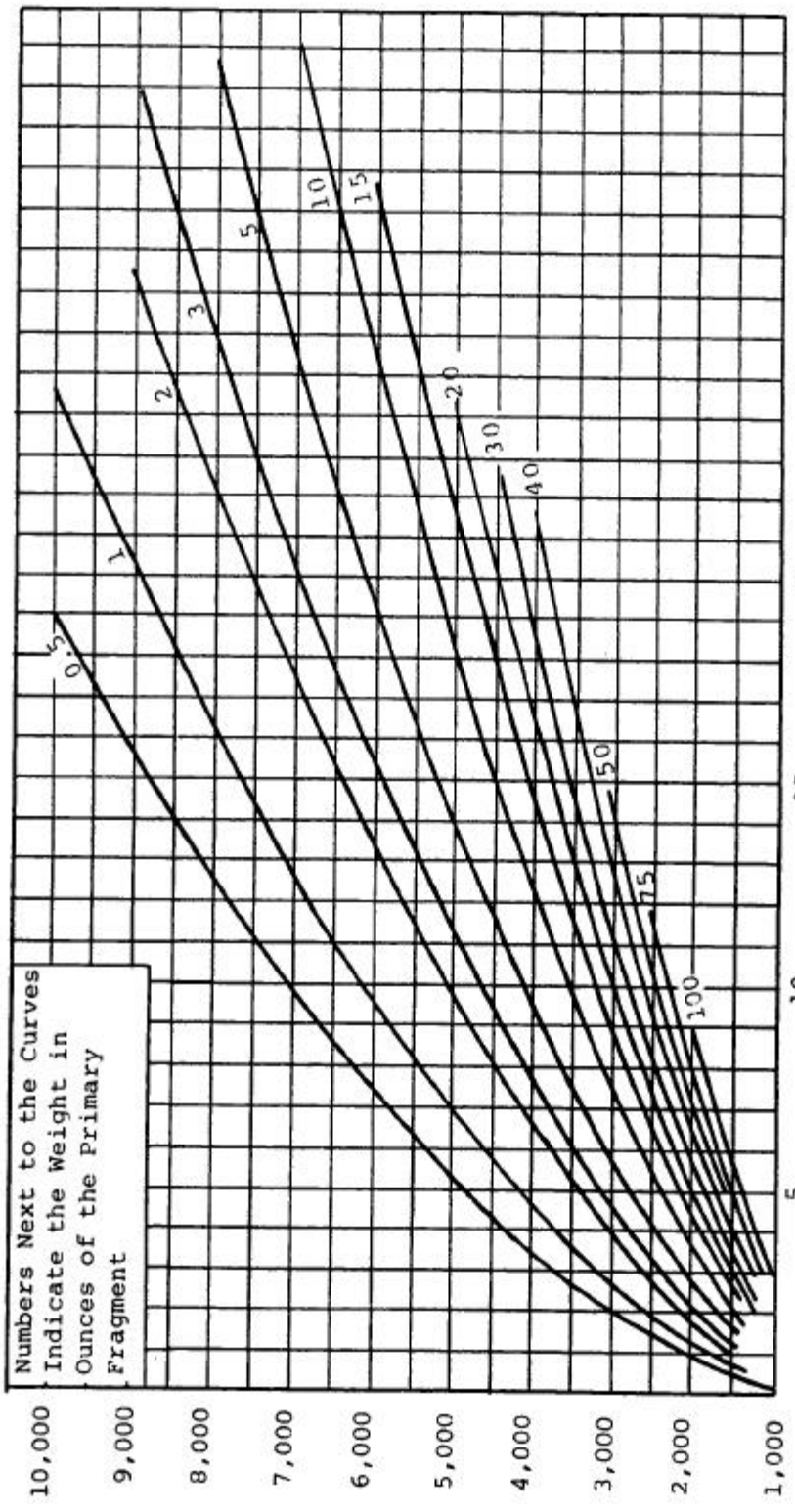

Figure 3-17. Fragment Penetration of 5,000 psi Concrete (Ref. 3-2)

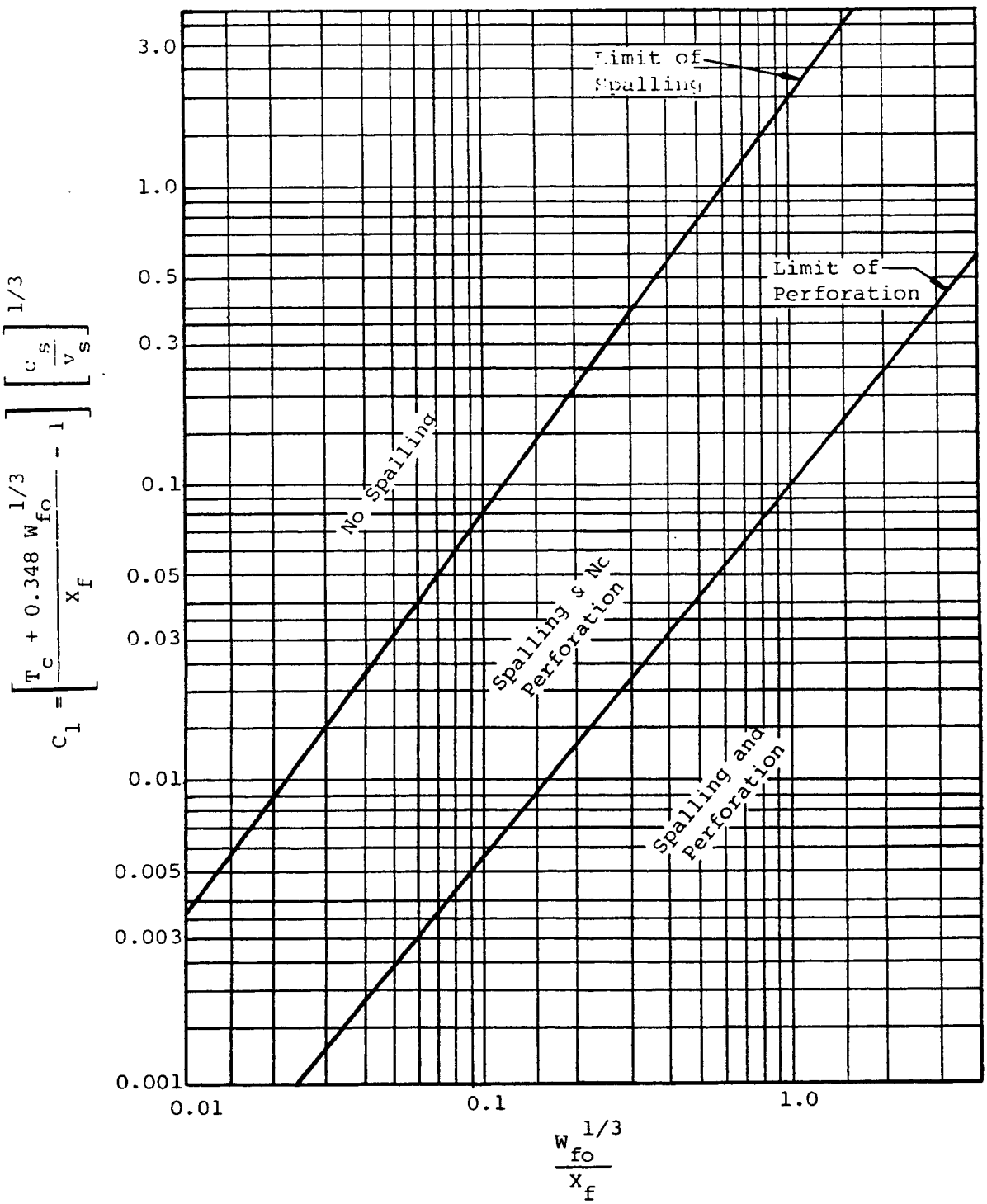

Figure 3-18. Limits of Concrete Spalling and Perforation (Ref. 3-2)

$$E_c = 33w^{1.5}\sqrt{f'_c} \quad \text{(psi)} \tag{3-22}$$

where

w = weight density of concrete, lb/ft^3

f'_c = static unconfined compressive strength of concrete, psi

Fragments which perforate a concrete element will have a residual velocity v_r which may endanger the receiver system. The magnitude of this velocity may be approximated from the expression which defines the velocity of the fragment at any time as it penetrates the concrete, i.e.,

$$\left(\frac{v_r}{v_s}\right)^{1.8} = 1 - \frac{T_c}{X_f} \tag{3-23}$$

where

T_c = thickness of concrete element, inches

v_r = residual velocity of the fragment as it leaves the concrete element, fps

Equation 3-23 applies when the depth of penetration is greater than 2 fragment diameters. If the depth of penetration is less than 2 fragment diameters, Ref. 3-45 recommends

$$\left(\frac{v_r}{v_s}\right)^{1.8} = 1 - \left(\frac{T_c}{X_f}\right)^2 \tag{3-24}$$

This handbook does not include procedures for estimating fragment diameters. If other information on fragment size is not available, it is recommended that Eq. 3-24 be used to estimate the fragment residual velocity. Plots of the ratio v_r/v_s against T_c/X_f are given in Fig. 3-19.

b. Other Fragments

To estimate the concrete penetration of metal

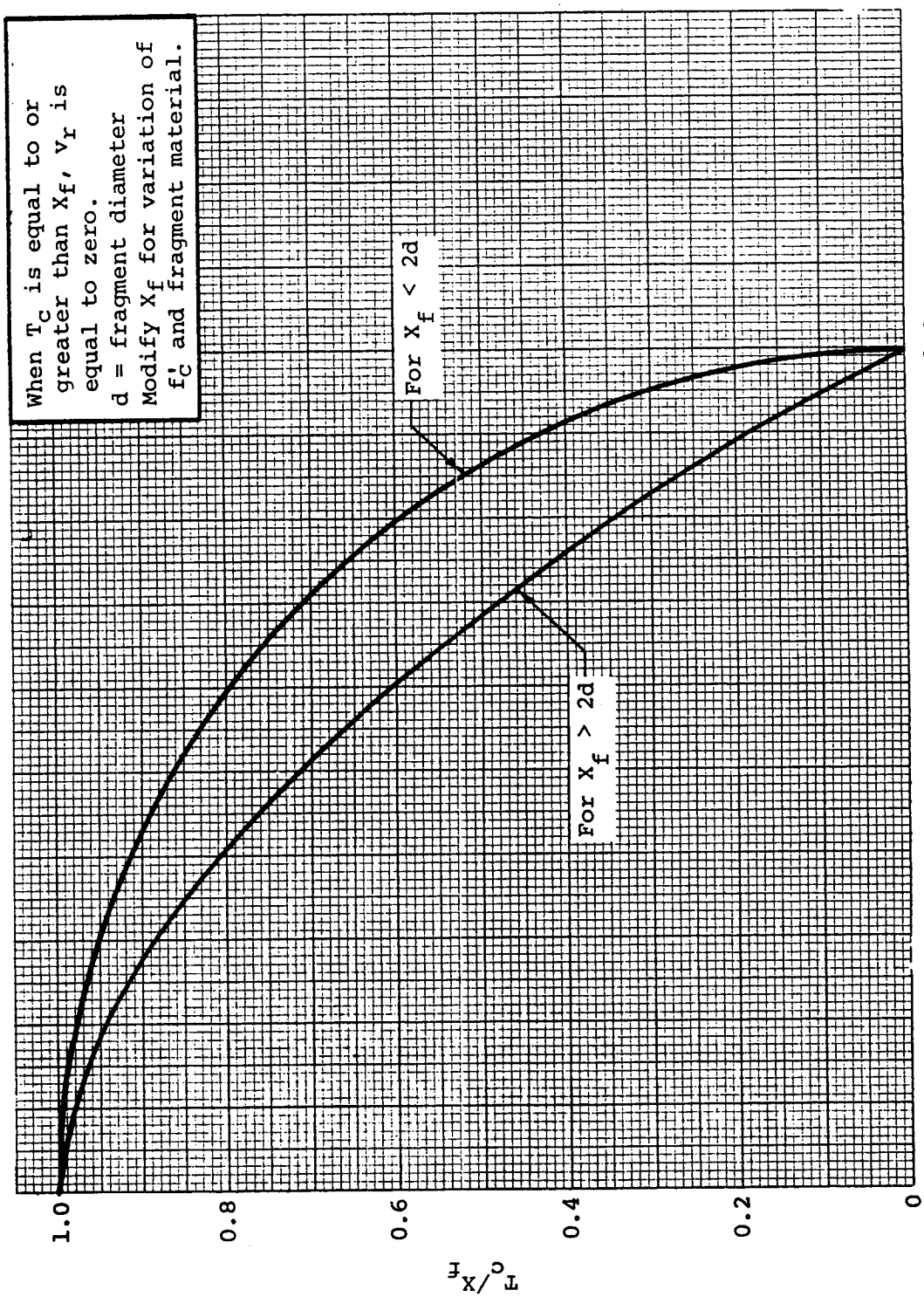

Figure 3-19. Residual Velocity of Primary Fragment After Perforation (Refs. 3-2 and 3-45)

fragments other than armor piercing, a procedure has been developed to relate the concrete penetrating capabilities of such fragments to those of armor-piercing fragments. This relationship is expressed in terms of relative metal hardness (the ability of the metal to resist deformation) and density, and is represented by constant C_2 in Eq. 3-25 (Ref. 3-2)

$$X_f' = C_2 X_f \tag{3-25}$$

where

X_f' = maximum penetration in concrete of metal fragments other than armor-piercing

The numerical values of C_2 for several of the more common casing metals are listed below:

Type of Metal	C_2
Armor-piercing steel	1.00
Mild steel	0.70
Lead	0.50
Aluminum	0.25

3.9 FIREBALL AND THERMAL ENVIRONMENT

The fireball and thermal environment resulting from an accidental explosion or deflagration can conceivably create as much damage as blast and fragmentation. An equally important function of a suppressive shield, therefore, is to suppress or attenuate the fireball and thermal environment to acceptable levels as well as blast and fragments.

The following expressions from Ref. 3-46 can be used to estimate the diameter and time of duration of a fireball in free air.

$$D_f = 9.56W^{0.325} \quad (3\text{-}26)$$

$$t_f = 0.196W^{0.349} \quad (3\text{-}27)$$

where

D_f = fireball diameter, ft

t_f = fireball time of duration, sec

W = charge weight, lb

Suppressive shields shall be designed to limit exposure of personnel to a critical heat flux value based on total time of exposure (Ref. 3-47). This value of heat flux shall be determined by

$$f = 0.62/t^{0.7423} \quad (3\text{-}28)$$

where

f = heat flux, cal/cm^2-sec

t = total time of exposure, sec

Unfortunately, there are no methods currently available with which attenuation of the fireball/thermal environment by a suppressive shield can be predicted. Until such time as proven analytical prediction methods do become available, demonstration of the ability of a suppressive shield design to satisfy the criteria of Eq. 3-28 will require an experimental program. Guidelines for planning and conducting the necessary experimental program are presented in Ref. 3-47.

All safety approved suppressive shields suppress the fireball to acceptable levels and can be used where fireball suppression is required.

3.10 ILLUSTRATIVE EXAMPLES

3.10.1 Shield Group 4 Airblast Loading Parameters

a. Given

The Shield Group 4 design features and charge weights shown in Table A-4. Summarizing, the interior dimensions for airblast calculations are 9.48 feet high x 9.66 feet wide x 14.56 feet long; the design charge weight is 9 pounds of 50/50 Pentolite; the proof charge weight is 11.25 pounds of 50/50 Pentolite.

The roof and wall are almost the same distance from the charge. Although the roof is a little closer than the wall, it is significantly stronger because of additional cross bracing and smaller panels. Therefore, this analysis will be concerned with the wall, since that is the most vulnerable member.

b. Find

The reflected pressure and the reflected impulse on the shield sidewall and the peak quasi-static pressure for both the design and proof charge weights.

c. Solution

First, convert the Pentolite charge weights to equivalent weights of TNT with Table 3-1.

Design : 9 lb x 1.129 = 10.16 lb TNT

Proof : 11.25 x 1.129 = 12.70 lb TNT

Next, determine the scaled distance from the charge, which is centrally located within the shield, to the nearest sidewall with Eq. 3-2, pg. 3-6. The distance R to the nearest wall for both charge weights is 9.66/2 = 4.83 ft.

Design : $Z = 4.83/(10.16)^{1/3} = 2.23$ ft/lb$^{1/3}$

Proof : $Z = 4.83/(12.70)^{1/3} = 2.07$ ft/lb$^{1/3}$

Enter Fig. 3-6 with these values for Z and read

Design : $\underline{P_r = 1150 \text{ psi}}$

$i_r/W^{1/3} = 6.8 \times 10^{-2}$ psi-sec/lb$^{1/3}$

$\underline{i_r = 147 \text{ psi-ms}}$

Proof : $\underline{P_r = 1480 \text{ psi}}$

$i_r/W^{1/3} = 7.3 \times 10^{-2}$ psi-sec/lb$^{1/3}$

$\underline{i_r = 170 \text{ psi-ms}}$

The charge to volume ratio is needed to compute the peak quasi-static pressure. The volume is

$$V = 9.48 \times 9.66 \times 14.56 = 1333.4 \text{ ft}^3$$

The charge to volume ratios are

Design : $10.16/1333.4 = 0.0076$ lb/ft^3

Proof : $12.70/1333.4 = 0.0095$ lb/ft^3

Enter Fig. 3-9 with these values of W/V and read

Design : $\underline{P_{qs} = 62 \text{ psi}}$

Proof : $\underline{P_{qs} = 70 \text{ psi}}$

3.10.2 Shield Group 4 Effective Vent Area Ratio

a. Given

The Shield Group 4 design as shown in Fig. A-5.

b. Find

The effective vent area ratio, α_e, for the shield.

c. Solution

The Group 4 panel cross section contains six layers of baffle elements as shown schematically in Fig. A-4. It can be determined from Fig. A-5 that the perforations of the 3/16-inch plates consist of 3/16-inch diameter holes on a 60 degree staggered pattern at 13/32-inch centers; see following sketch.

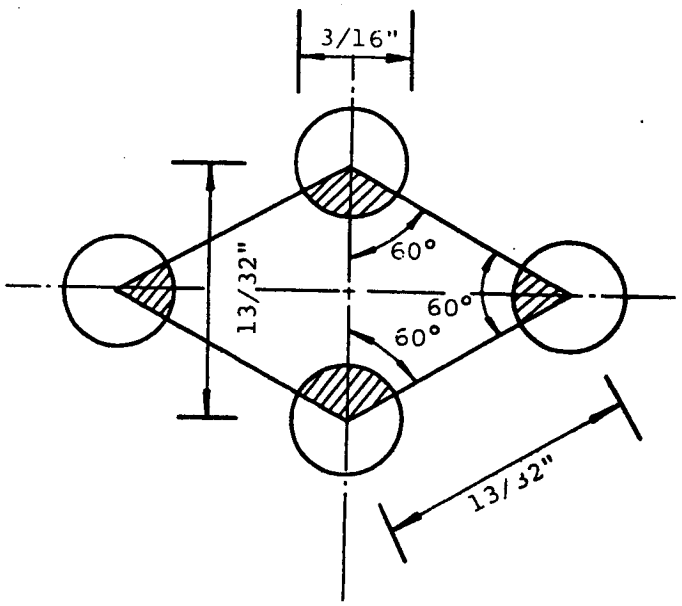

Group 4 Shield Panel Plate Perforation Pattern

Referring to the sketch, the ratio of the perforations to the solid plate can be found to be

$$\alpha = \frac{0.25\pi(0.1875)^2}{(4)(0.5)(0.406\sin 60°)(0.203)} = 0.193$$

The exposed perforated plate area between columns and mounting bracket angles can be estimated to be 45 x 111 inches and the gross panel area can be taken as 55 x 111 inches; see Fig. A-5. The vent area ratio for the perforated plate panel is, therefore,

$$\alpha_1 = \frac{A_{v1}}{A_w} = \frac{(0.193)(4995)}{6105} = 0.158$$

The vent area for the nested angles can be determined by

$$A_v = n\ell a/N$$

as shown in Fig. 3-7. The nested angle geometry is illustrated below.

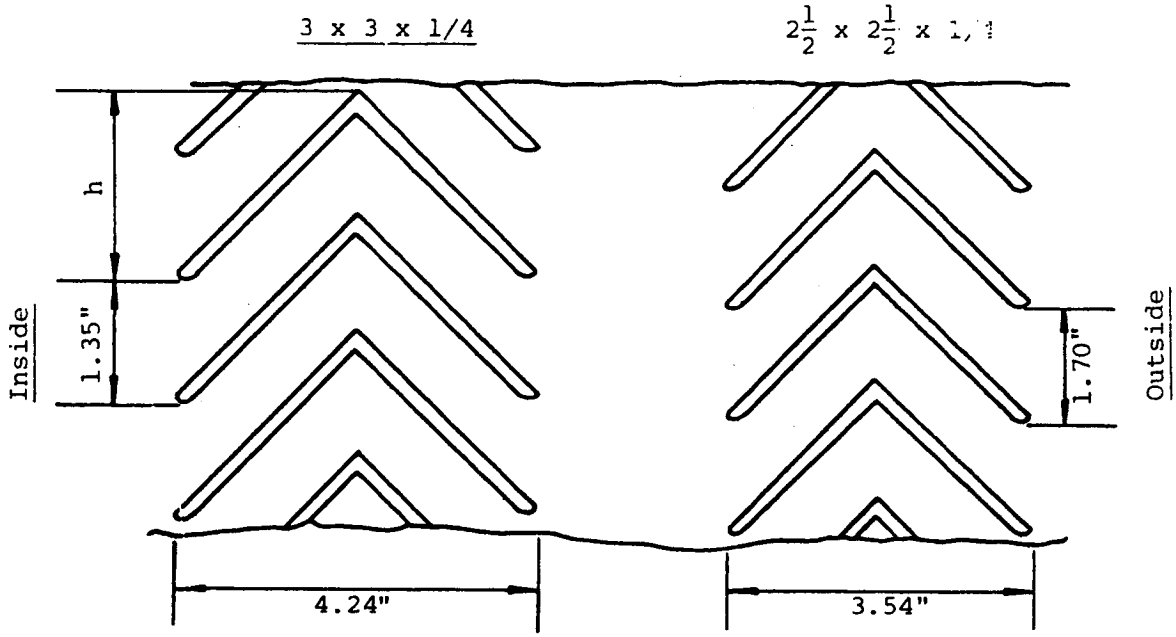

Group 4 Shield Panel Nested Angle Geometry

From Fig. A-5d, it can be seen that one half-panel has 42 stacked 3 x 3 x 1/4 angles; this makes the number of openings n = 41 for a half-panel and n = 82 for the full panel. The exposed length of the angles is 45 inches as shown on Fig. A-5d. The projected width of the 3 x 3 x 1/4 angles is

$$h = 3\sin 45° = 2.12 \text{ inches}$$

and the opening is 1.35 inches as shown on the above sketch. The number of openings per projected width is 2.12/1.35 = 1.57, which is near 2, so take N = 4 as per Fig. 3-7. The distance between the angles is

$$a = 1.35\sin 45° = 0.95 \text{ inches}$$

The vent area for the 3 x 3 x 1/4 angles is, therefore,

$$A_{v2} = (82)(45)(0.95)/4 = 876.4 \text{ in.}^2$$

It can be determined from Fig. A-5 that L = 111 inches and M = 55 inches, resulting in $A_w = (111)(55) = 6105$ in.^{2} and

$$\alpha_2 = A_{v2}/A_w = 876.4/6105 = 0.144$$

Going through the above steps for the 2-1/2 x 2-1/2 x 1/4 angle geometry leads to

$$\alpha_3 = \frac{A_{v3}}{A_w} = \frac{(66)(45)(1.20)/2}{6105} = 0.292$$

As may be seen in Fig. A-4, there are four perforated plates (α_1) and one layer each of the 3 x 3 and 2-1/2 x 2-1/2 angles (α_2, α_3). The effective vent area ratio by Eq. 3-5, pg. 3-17 is

$$\frac{1}{\alpha_e} = \frac{4}{0.158} + \frac{1}{0.144} + \frac{1}{0.292} = 35.7$$

$$\underline{\underline{\alpha_e = 0.03}}$$

The effective vent area ratio calculated above is actually for one full panel of the Shield Group 4 design. Due to the way α_e was calculated, however, with the wall area A_w taken as center to center of the columns, $\alpha_e = 0.03$ for the entire shield. The venting area blocked by the longitudinal roof beam (see Fig. A-6a) could be subtracted from the overall vented area (the walls and roof), but the effect on α_e is negligible in this case.

3.10.3 Shield Group 4 Design Blowdown Time and External Pressure

a. Given

The Shield Group 4 design as shown in Fig. A-5.

b. Find

The blowdown time and the incident overpressure at a point 19 feet from the exterior shield wall for the design charge weight.

c. Solution

The design quasi-static pressure found in paragraph 3.10.1 above is 62 psi. Find $\bar{P}$ with which to enter Fig. 3-10.

$$\bar{P} = \frac{P_{qs} + P_o}{P_o} = \frac{62 + 15}{15} = 5.13$$

Enter Fig. 3-10 with $\bar{P} = 5.13$ and find

$$\frac{t_b a_o \alpha_e A_i}{V} = 0.77$$

Take

a_o = 1117 fps (par. 3.5.2)

α_e = 0.03 (par. 3.10.2)

V = 1333.4 ft^3 (par. 3.10.1)

$A_i = 2(9.48)(14.56) + 2(9.48)(9.66) + (9.66)(14.56)$
$= 599.9\ ft^2$

Then,

$$t_b = \frac{(0.77)(1333.4)}{(1117)(0.03)(599.9)} = 0.051 \text{ sec}$$

$\underline{\underline{t_b = 51 \text{ ms}}}$

The peak incident pressure 19 feet outside the shield can be found with Eq. 3-7, pg. 3-27. Take R = 4.83 + 19 = 23.83, say 24 ft. Then

$$Z = 24/(10.16)^{1/3} = 11.08 \text{ ft/lb}^{1/3}$$

for the design charge weight. Take

$$X = (9.66 \times 14.56)^{1/2} = 11.86 \text{ ft}$$

and $\alpha_e = 0.03$ as before. From Eq. 3-7,

$$P_{so} = 957\left(\frac{1}{11.08}\right)^{1.66}\left(\frac{24}{11.86}\right)^{0.27}\left(0.03\right)^{0.64}$$

$$\underline{\underline{P_{so} = 2.3 \text{ psi}}}$$

3.10.4 Primary Fragment Mass and Velocity

a. Given

A cylindrical cased explosive charge loaded with TNT. The charge weight W is 0.191 lb; the case weight W_c is 4.2 lb; the case thickness t is 0.5 inches; and the internal case diameter d_i is 2.0 inches.

b. Find

The weight and initial velocity of the largest expected primary fragment.

c. Solution

The weight of the largest expected primary fragment can be estimated with Eq. 3-9, pg. 3-30. Go to Table 3-2 and find that the constant B = 0.0779 for TNT. Then, calculate

$$C = \left[(0.0779)(0.5)^{5/6}(2.0)^{1/3}(1 + 0.5/2.0)\right]^2$$

$$C = 0.00474 \text{ lb}$$

With Eq. 3-9, estimate the largest primary fragment weight to be

$$W_f = 0.00474\left[\ln\left(\frac{4.2}{2 \times 0.00474}\right)\right]^2$$

$$\underline{\underline{W_f = 0.176 \text{ lb}}}$$

The primary fragment initial velocity can be estimated with Eq. 3-10, pg. 3-30. First, find the Gurney energy

constant for TNT in Table 3-3 to be 7780 fps. Then, from Eq. 3-10,

$$v_o = 7780\left[\frac{0.191/4.2}{1 + 0.191/(2)(4.2)}\right]^{1/2}$$

$$\underline{\underline{v_o = 1640 \text{ fps}}}$$

3.10.5 Secondary Fragment Velocity

a. Given

A front roller support axle for the 105-mm projectile fuze insert and torquing machinery would be a typical secondary fragment. The axle is located side-on to the projectile; is cylindrical in shape with a circular area of 0.194 in^2; has a length of 2.74 inches and weighs 0.15 lb. The equivalent spherical charge of Comp B has a radius R_e of 2.57 inches and the range R from the center of the equivalent charge to the edge of the axle is 3.89 inches.

b. Find

The initial velocity of the axle as a secondary fragment.

c. Solution

The initial velocity will be estimated with Eq. 3-11, pg. 3-32. Establish that

$$g_s = \pi/4 = 0.785$$

$$M = 0.15/386 = 0.000389 \text{ lb-sec}^2/\text{in}$$

$$R_e/R = 2.57/3.89 = 0.66$$

The estimated initial velocity of the secondary fragment by Eq. 3-11 is

$$v_{os} = \frac{(0.194)(2.57)(0.785)}{0.000389}\left[(0.556)(0.66) + (2.75)(0.66)^2\right]$$

$$\underline{\underline{v_{os} = 1575 \text{ fps}}}$$

3.10.6 Fragment Impact on Shield Group 3 Wall Panel

a. Given

The compact mild steel primary fragment predicted in paragraph 3.10.4 striking the Shield Group 3 wall panel as shown in the following sketch.

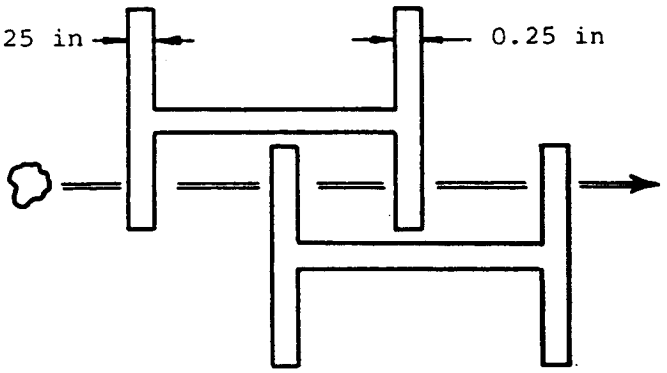

Shield Group 3 Wall Panel Geometry

The fragment is blunt and of roughly cylindric shape so that the length to diameter ratio is L/D = 1.0. The fragment threat parameters for the first element are

W_s = 0.176 lb

v_s = 1640 fps

θ = 0°

ϕ = 0°

t = 0.25 inches

A_p = 0.674 in^2

L = 0.926 inches

b. Find

The penetration depth of the impacting fragment.

c. Solution

To determine the constants used for estimating the limit velocity for the first panel, the ratio $t/(R\sqrt{A_p})$ is calculated. The perforation factor R is one for solid plate.

$$\frac{t}{R\sqrt{A_p}} = \frac{0.25}{1.0\sqrt{0.674}} = 0.305$$

Using Table 3-5 and Eq. 3-12, pg. 3-39, the limit velocity is

$$v_\ell = \frac{1414}{\sqrt{0.176}} (0.674)^{0.295} (0.25\sec 0°)^{0.910}$$

$$v_\ell = 849 \text{ fps}$$

To calculate the residual velocity, first find

$$x = \frac{v_s}{v_\ell} - 1 = \frac{1640}{849} - 1 = 0.932$$

Then, using Eq. 3-14, pg. 3-41 and the constants in Table 3-6, the residual velocity is

$$v_r = 849\beta\left[\frac{1.12(0.932)^2 + 0.52(0.932) + 1.29(0.932)^{1/2}}{1.932}\right]$$

$$v_r = 1188\beta \text{ fps}$$

The term β could be set to unity to obtain a quick overestimate of residual velocity. However, to get a more accurate result, β is calculated as defined under Eq. 3-14. (Take the density of solid steel plate as 0.284 lb/in^3).

$$\beta = \frac{1}{[1 + (0.284)(0.674)(0.25)/0.176]^{1/2}} = 0.887$$

and the residual velocity becomes 1050 fps.

To estimate the residual weight, first determine the critical angle for shatter ϕ_c from Eq. 3-15, pg. 3-43.

$$\phi_c = \arcsin\left[\frac{1640\cos 0°}{18010}\right] = 5.22°$$

Since $\phi < \phi_c$, the impact is considered flat, and the critical velocity for shatter must be found with Eq. 3-16, pg. 3-43.

$$v_{cr} = 2000/\cos 0° = 2000 \text{ fps}$$

Since $v_s < v_{cr}$, the velocity is insufficient for shatter, and the deformation mass loss equations must be used. The first step is to calculate the correlational velocity v_{co} from Eq. 3-18, pg. 3-44.

$$v_{co} = \frac{1640}{1 + \frac{\frac{\cos 0°}{(0.6)(0.25)(0.284)(0.674)}}{0.176} + 0.15}$$

$$v_{co} = 391 \text{ fps}$$

This velocity is less than the threshold velocity for any deformation to occur (700 fps), so the residual mass is unchanged, i.e.,

$$W_r = W_s$$

The fragment threat parameters for the second element thus become

$W_s = 0.176$ lb

$v_s = 1050$ fps

$\theta = 0°$

$\phi = 0°$

$t = 0.25$ inches

$A_p = 0.674$ in^2

$L = 0.926$ inches

All parameters remain unchanged from the initial conditions, except for the striking velocity, v_s. The striking velocity does not enter the limit velocity expression, Eq. 3-12, pg. 3-39, so v_ℓ is the same as for the first element. Determine the residual velocity quantity

$$x = \frac{1050}{849} - 1 = 0.237$$

Then, since $\beta = 0.887$ as before, the residual velocity after perforating the second element is

$$v_r = (849)(0.887)\left[\frac{1.12(0.237)^2 + 0.52(0.237) + 1.29(0.237)^{1/2}}{1.237}\right]$$

$v_r = 496$ fps

Since the velocity of the fragment leaving the second element is less than the limit velocity of the next element, $v_r = 496$ fps $< v_\ell = 849$ fps, the fragment will be defeated by the third element of the shield wall panel shown in the sketch on pg. 3-60.

3.10.7 Fragment Impact on Shield Group 4 Panel

a. Given

The secondary fragment predicted in paragraph 3.10.5 striking the Shield Group 4 panel shown in Fig. A-4. The fragment is assumed to strike end-on with zero obliquity. The pertinent features of the panel section shown in Fig. A-4 are summarized in the following table (pg. 3-64).

The fragment threat parameters for the first element are

$W_s = 0.15$ lb

$v_s = 1575$ fps

$\theta = 0°$

$\phi = 0°$

Shield Group 4 Panel Features

Element No.	t (in)	θ (deg)	Type Element
1	0.188	0	Perforated
2	0.25	45	Solid
3	0.25	45	Solid
4	0.188	0	Perforated
5	0.188	0	Perforated
6	0.188	0	Perforated
7	0.25	45	Solid
8	0.25	45	Solid

$t = 0.188$ inch

$A_p = 0.194$ in^2

$L = 2.74$ inches

$D = 0.50$ inch

b. Find

The depth to which the fragment penetrates the panel.

c. Solution

First, determine R for the first element, which is a perforated plate. It was found in paragraph 3.10.2 that the vent area ratio α for the Group 4 perforated plate was 0.193. From Fig. 3-16, $R = 0.54$ for $\alpha = 0.193$ and a hexagonal array (Eq. 3-13, pg. 3-41, could also be used to determine R). Since $L/D = 2.74/0.50 = 5.5$, use the long rod ($L/D > 5$) constants from Table 3-5 to find the limit velocity. Recall that R^2A_p is substituted for A_p in Eq. 3-12, pg. 3-39, for perforated plates.

$$v_\ell = \frac{1261}{\sqrt{0.15}} [(0.54)^2(0.194)]^{0.427}(0.188\sec 0°)^{0.647}$$

$$v_\ell = 324 \text{ fps}$$

The quantity x needed to compute the residual velocity is

$$x = \frac{1575}{324} - 1 = 3.86$$

and the residual velocity from Eq. 3-14, pg. 3-41, with the long rod (L/D > 5) constants from Table 3-6 is

$$v_r = (324)(1)\left[\frac{1.1(3.86)^2 + 0.80(3.86) + 1.45(3.86)^{1/2}}{4.86}\right]$$

$$= 1488 \text{ fps}$$

Since $\phi = 0°$, the impact is flat. The critical velocity for shatter, Eq. 3-16, pg. 3-43, is

$$v_{cr} = 2000/\cos 0° = 2000 \text{ fps}$$

and $v_s < v_{cr}$. Compute the correlational velocity with Eq. 3-18, pg. 3-44. The density γ in Eq. 3-18 is reduced to take account of the perforations in the plate, i.e., $\gamma = (0.284)(0.807) = 0.229 \text{ lb/in}^3$.

$$v_{co} = \frac{1575}{1 + \frac{\cos 0°}{\frac{(0.6)(0.188)(0.229)(0.194)}{0.15} + 0.15}}$$

$$v_{co} = 244 \text{ fps}$$

Since $v_{co} < 700$ fps, no mass loss occurs.

The fragment threat parameters for the second element are

$W_s = 0.15$ lb

$v_s = 1488$ fps

$\theta = 45°$

$\phi = 45°$

$t = 0.25$ inch

$A_p = 0.194\ in^2$

$L/D = 5.5$

$R = 1.0$

The limit velocity for the second element with Eq. 3-12, pg. 3-39, and the long rod constants from Table 3-5 thus becomes

$$v_\ell = \frac{1261}{\sqrt{0.15}} (0.194)^{0.427} (0.25\sec 45°)^{0.647}$$

$$v_\ell = 825 \text{ fps}$$

Calculate the residual velocity as before.

$$x = \frac{1488}{825} - 1 = 0.80$$

$$v_r = (825)(1)\left[\frac{1.1(0.80)^2 + 0.80(0.80) + 1.45(0.80)^{1/2}}{1.80}\right]$$

$$v_r = 1210 \text{ fps}$$

The critical angle for shatter is

$$\phi_c = \arcsin\left[\frac{1488\cos 45°}{18010}\right] = 3.35°$$

Since $\phi > \phi_c$, the impact is a corner or edge impact, and the fragment is in the deformation mass loss mode. The correlational velocity is

$$v_{co} = \frac{1488}{1 + \frac{\frac{\cos 45°}{0.6(0.25)(0.284)(0.194)}}{0.15} + 0.15}$$

$$v_{co} = 335 \text{ fps}$$

The correlational velocity is too small for any mass loss, i.e., $v_{co} < 700$ fps. Since the remaining elements are identical to

either the first or second element, and since the striking velocities must be less than those for the first two, the correlational velocities for all remaining elements will also be too small for any mass loss. Therefore, the mass of this fragment remains unchanged after every impact.

Consequently, only residual velocity calculations need be repeated until it is found that the residual velocity after perforating an element is less than the limit velocity of the next element. The results of these calculations are summarized below.

Element No. 3

v_s = 1210 fps

v_ℓ = 825 fps

x = 0.47

v_r = 906 fps

Element No. 4

v_s = 906 fps

v_ℓ = 324 fps

x = 1.80

v_r = 804 fps

Element No. 5

v_s = 804 fps

v_ℓ = 324 fps

x = 1.48

v_r = 700 fps

Element No. 6

v_s = 700 fps

v_ℓ = 324 fps

x = 1.16

v_r = 595 fps

Recall that Element No. 7 has the same features as Element Nos. 2 and 3, i.e., a limit velocity of 825 fps. Since the striking velocity on Element No. 7 is only 595 fps, it is predicted that the fragment is stopped at Element No. 7.

3.11 LIST OF SYMBOLS

a	Equation constant
a_o	Speed of sound in air at sea level (ft/sec)
A	Open area of louvre (in^2)
A_i	Internal surface area of suppressive shield (ft^2)
A_o	Equation constant
A_p	Area of fragment (in^2)
A_v	Vent area (in^2)
A_{vi}	Vent area for i-th layer of wall (in^2)
A_w	Area of wall (in^2)
A_{wi}	Area of i-th layer of wall (in^2)
b	Equation constant
B	Explosive constant ($lb^{1/2}$ inches $^{-7/6}$)
c	Equation constant
c_p	Velocity of sound in metal plate (ft/sec)
c_s	Dilatational velocity of elastic wave through concrete (ft/sec)
$C, C_1, C_2, C_3, \ldots,$	Equation constants
d_c	Charge diameter (inches)
d_{co}	Diameter of core element (inches)
d_i	Inside diameter (inches)
d_p	Diameter of perforations (inches)
D	Diameter (inches)
D_f	Fireball diameter (ft)
e_t	TNT equivalent factor
E_c	Modulus of elasticity of concrete (psi)
f	Heat flux (cal/cm^2-sec)
f'_c	Static unconfined compressive strength of concrete (psi)
g	Equation constant (Table 3-4)
g_s	Shape factor
h	Projected width (inches)
h_p	Center-to-center distance between perforations (inches)

i_r	Reflected pressure impulse (psi-sec)
i_s	Positive incident impulse (psi-sec)
ℓ,L	Length (inches)
m	Equation constant
M	(1) Mass of secondary fragment (lb-sec^2/in) (2) Panel width (inches)
n	(1) Number of items or openings (2) Number of different types or sizes of panel members (3) Equation constant
N	Equation constant
p(t)	Pressure as a function of time (psi)
P_o	Ambient pressure at sea level (psi)
P_{qs}	Peak quasi-static pressure (psi)
P_r	Peak reflected overpressure (psi)
P_{so}	Peak positive incident pressure (psi)
P_{so}^-	Peak negative incident pressure (psi)
R	(1) Distance from the center of the explosive source to the point of interest (ft, inches) (2) Perforation factor
R_e	Radius of spherical explosive source (inches)
t	(1) Time (sec) (2) Thickness (inches)
t_a	Shock front arrival time (sec)
t_b	Duration of quasi-static pressure (sec)
t_f	Duration of fireball (sec)
t_o	Duration of positive pressure pulse (sec)
t_o^-	Duration of negative pressure pulse (sec)
t_r	Duration of positive reflected pressure (sec)
T_c	Thickness of concrete element (inches)
u_s	Incident particle velocity (ft/sec)
U	Airblast shock front velocity (ft/sec)
v_{co}	Correlational velocity (ft/sec)
v_{cr}	Critical velocity (ft/sec)
v_ℓ	Ballistic limit velocity (ft/sec)

v_o	Initial primary fragment velocity (ft/sec)
v_{os}	Initial velocity of secondary fragment (in/sec)
v_r	Residual velocity of fragment (ft/sec)
v_s	Striking velocity of fragment (ft/sec)
V	Volume (ft^3)
w	Unit weight of concrete (lb/ft^3)
W	Charge weight of explosive (lbs)
W_c	Weight of casing (lbs)
W_{c1}, W_{c2}	Weight of sandwich plates (lbs)
W_{co}	Weight of core element (lbs)
W_e	Effective charge weight in pounds of TNT
W_f	Weight of fragment (lbs)
W_{fo}	Weight of fragment (oz)
W_r	Residual weight of fragment (lbs)
W_s	Striking weight of fragment (lbs)
W_{TNT}	Equivalent charge weight of TNT (lbs)
x	Equation parameter
X	Characteristic length of structure (ft)
X_f	Maximum penetration depth in concrete of armor piercing fragment (inches)
X'_f	Maximum penetration depth in concrete of other than armor piercing fragment (inches)
Z	Scaled distance ($ft/lb^{1/3}$)
α_e	Vent area ratio of shield
α_i	Vent area ratio for single layer of multiple layer wall
β	Equation coefficient
γ	Density of target plate (lb/in^3)
θ	Angle of obliquity (degrees)
λ	Scalar multiplier
ϕ	Orientation angle (degrees)
ϕ_c	Critical orientation angle (degrees)
$\sqrt{2E'}$	Gurney energy constant (ft/sec)

3.12 REFERENCES

3-1 Engineering Design Handbook: Explosions in Air, Part I, AMC Pamphlet 706-181, Headquarters U.S. Army Materiel Command, Latest Edition. (U)

3-2 Structures to Resist the Effects of Accidental Explosions, TM5-1300, Department of the Army, Washington, D.C., June 1969. (U)

3-3 Crawford, R.E., Higgins, C.J. and Bultmann, E.H., The Air Force Manual for Design and Analysis of Hardened Structures, AFWL TR 74-102, Air Force Weapons Laboratory, Kirtland AFB, N.M., October 1974. (U)

3-4 Tomlinson, W.R., Jr. and Sheffield, O.E., Engineering Design Handbook, Properties of Explosives of Military Interest, AMC Pamphlet No. 706-177, Headquarters, U.S. Army Materiel Command, January 1971. (U)

3-5 Safety Criteria for Modernization and Expansion Projects, DRCPM-PBM Memorandum No. 385-3, Latest Edition. (U)

3-6 Napadensky, H. and Swatosh, J., TNT Equivalency of Black Powder, (Vol I & II) IITRI TR J6265-3, IIT Research Institute, Chicago, Ill., September 1972. (U)

3-7 Swatosh, J. and Napadensky, H., TNT Equivalency N-5 Slurry and Paste, IITRI TR J6278, IIT Research Institute, Chicago, Ill., September 1972. (U)

3-8 Swatosh, J. and Napadensky, H., TNT Equivalency of Nitroglycerine, IITRI TR J6312, IIT Research Institute, Chicago, Ill., September 1973. (U)

3-9 Napadensky, H. and Swatosh, J., TNT Equivalency of Large Charges of Black Powder, IITRI TR J6289-4, IIT Research Institute, Chicago, Ill., February 1974. (U)

3-10 Napadensky, H., Swatosh, J., Humphreys, A., and Rindner, R., TNT Equivalency Three Pyrotechnic Composition, PA TR 4628, Picatinny Arsenal, Dover, N.J., June 1974. (U)

3-11 Levmore, S., Air Blast Parameters and Other Characteristics of Nitroguanidine and Guanidine Nitrate, PA TR 4865, Picatinny Arsenal, Dover, N.J., November 1975. (U)

3-12 Swatosh, J., et al, and Levmore, S., Blast Parameters of Lead Styphnate, Lead Azide, and Tetracene, PA TR 4900, Picatinny Arsenal, Dover, N.J., December 1974. (U)

3-13 Swatosh, J., et al, and Price, P., TNT Equivalency of Ml Propellant (Bulk), PA TR 4885, Picatinny Arsenal, Dover, N.J., December 1975. (U)

3-14 Swatosh, J., Cook, J., and Price, P., Blast Parameters of M26E1 Propellant, PA TR 4901, Picatinny Arsenal, Dover, N.J., December 1976. (U)

3-15 Kingery, C.N., Air Blast Parameters Versus Distance for Hemispherical TNT Surface Bursts, BRL Report No. 1344, Aberdeen Proving Ground, Maryland, September 1966. (U)

3-16 Petes, J., "Blast and Fragmentation Characteristics," Annals of the New York Academy of Sciences, Vol. 152, Article 1, October 1968, pp. 283-317. (U)

3-17 Swisdak, M.M., Jr., Explosion Effects and Properties: Part I - Explosion Effects in Air, NSWC/WOL/TR 75-116, Naval Surface Weapons Center, White Oak, Silver Spring, Maryland, October 1975. (U)

3-18 Gregory, F.H., Analysis of the Loading and Response of a Suppressive Shield When Subjected to an Internal Explosion, Minutes of the 17th Explosive Safety Seminar, Denver, Colorado, September 1976. (U)

3-19 Esparza, E.D., Baker, W.E., and Oldham, G.A., Blast Pressures Inside and Outside Suppressive Structures, EM-CR-76042, Report No. 8, Edgewood Arsenal, Aberdeen Proving Ground, Maryland, December 1975. (U)

3-20 Kingery, C.N., Schumacher, R.N., and Ewing, W.O., Jr., Internal Pressures from Explosions in Suppressive Structures, BRL Interim Memorandum Report No. 403, Aberdeen Proving Ground, Maryland, June 1975. (U)

3-21 Schumacher, R.N., Kingery, C.N., and Ewing, W.O., Jr., Airblast and Structural Response Testing of a 1/4 Scale Category 1 Suppressive Shield, BRL Memorandum Report No. 2623, Aberdeen Proving Ground, Maryland, May 1976. (U)

3-22 Weibull, H.R.W., Pressures Recorded in Partially Closed Chambers at Explosion of TNT Charges, Annals of the New York Academy of Sciences, 152, Art. 1, pp. 356-361, October 1968. (U)

3-23 Keenan, W.A. and Tancreto, J.E., Blast Environment from Fully and Partially Vented Explosions in Cubicles, Technical Report R828, Civil Engineering Laboratory, Naval Construction Battalion Center, Port Hueneme, California, November 1975. (U)

3-24 Zilliacus, S., Phyillaier, W.E., and Shorrow, P.K., The Response of Clamped Circular Plates to Confined Explosive Loadings, Naval Ship R&D Center Report 3987, NSRDC, Bethesda, Maryland, February 1974. (U)

3-25 Kinney, G.F. and Sewell, R.G.S., Venting of Explosions, Naval Weapons Center, NWC Technical Memorandum 2448, China Lake, California, July 1974. (U)

3-26 Baker, W.E. and Oldham, G.A., Estimates of Blowdown of Quasi-Static Pressures in Vented Chambers, EM-CR-76029, Report No. 2, Edgewood Arsenal, Aberdeen Proving Ground, Maryland, November 1975. (U)

3-27 Oertel, F.H., Jr., Evaluation of Simple Models for the Attenuation of Shock Waves by Vented Plates, BRL Report No. 1906, Aberdeen Proving Ground, Maryland, August 1976. (U)

3-28 Proctor, J.F. and Filler, W.S., A Computerized Technique for Blast Loads from Confined Explosions, 14th Annual Explosives Safety Seminar, New Orleans, Louisiana, 8-10 November 1972, pp. 99-124. (U)

3-29 Proctor, J.F., Internal Blast Damage Mechanisms Computer Program, 61 JTCG/ME-73-3, Joint Technical Coordinating Group for Munitions Effectiveness, April 1973. (U)

3-30 Proctor, J.F., Blast Suppression/Predictive Model, WBS 4333, Monthly Technical Report, November 1975, Naval Surface Weapons Center, White Oak, Silver Spring, Maryland. (U)

3-31 Lasseigne, A.H., Static and Blast Pressure Investigation for the Chemical Agent Munition Demilitarization System: Sub-Scale, Rpt. EA-FR-4C04, November 30, 1973. (U)

3-32 Koger, D.M. and McKown, G.L., Category 5 Suppressive Shield Test Report, EM-TR-76001, Edgewood Arsenal, Aberdeen Proving Ground, Maryland, October 1975. (U)

3-33 Study of Suppressive Structures Applications to an 81 mm Automated Assembly Facility, Report EA 1002, Edgewood Arsenal, Aberdeen Proving Ground, Maryland, 16 April 1973. (U)

3-34 81 mm Suppressive Shielding Technical Data Package, Report EA-4E33, Edgewood Arsenal, Aberdeen Proving Ground, Maryland, January 1974. (U)

3-35 Final Report Application of Suppressive Structure Concepts to Chemical Agent Munition Demilitarization System (CAMDS), Report EA-FR-2B02, Edgewood Arsenal, Aberdeen Proving Ground, Maryland, July 27, 1973. (U)

3-36 Schumacher, R.N. and Ewing, W.O., Jr., Blast Attenuation Outside Cubical Enclosures Made Up of Selected Suppressive Structures Panel Configurations, BRL Memorandum Report No. 2537, Aberdeen Proving Ground, Maryland, September 1975. (U)

3-37 Hoggatt, C.R. and Recht, R.F., Fracture Behavior of Tubular Bombs, J. Appl. Physics, Vol. 39, No. 3, February 1968, pp. 1856-1862. (U)

3-38 Mott, N.F., The Theory of Fragmentation, AC 3348 (British), January 1943. (U)

3-39 Mott, N.F., A Theoretical Formula for the Distribution of Weights of Fragments, AC 3742 (British) March 1943. (U)

3-40 Johnson, C. and Moseley, J.W., Preliminary Warhead Terminal Ballistic Handbook Part I, Terminal Ballistic Effects, NWL Report No. 1821, NAVWEPS Report No. 7673, U.S. Naval Weapons Laboratory, Dahlgren, Virginia, March 1964. (U)

3-41 Kennedy, J.E., Explosive Output for Driving Metal, in Behavior and Utilization of Explosives in Engineering Design, ASME and Univ. of New Mexico, March 1972, Albuquerque, New Mexico. (U)

3-42 Henry, I.G., The Gurney Formula and Related Approximations for the High Explosive Deployment of Fragments, PUB-189, Hughes Aircraft Co., AD813398, April 1967. (U)

3-43 Kennedy, R.P., A Review of Procedures for the Analysis of Design of Concrete Structures to Resist Missile Impact Effects, Nuclear Engineering and Design, Vol. 37, 1976, pp. 183-203. (U)

3-44 Ricchiazzi, A.J. and Barb, J.C., A Tentative Model for Predicting the Terminal Ballistic Effects of Blunt Fragments Against Single and Spaced Targets, A Comparison of Predicted and Experimental Results, BRL Memorandum Report 2578, Aberdeen Proving Ground, Maryland, January 1976. (U)

3-45 Headey, John, et al, Primary Fragment Characteristics and Impact Effects on Protective Barriers, PA TR 4903, Picatinny Arsenal, Dover, N.J., December 1975. (U)

3-46 Rakaczky, J.A., The Suppression of Thermal Hazards from Explosions of Munitions: A Literature Survey, BRL Interim Memorandum Report No. 377, Aberdeen Proving Ground, Maryland, May 1975. (U)

3-47 Shields, Operational for Ammunition Operations, Criteria for Design of, and Tests for Acceptance, Mil Std 398, U.S. Government Printing Office, Washington, D.C., 5 November 1976. (U)